Separation Science and Technology
Publication details, including instructions for authors and subscription information:
http://www.informaworld.com/smpp/title~content=t713708471

Pressure Effects in Adsorbers and Adsorptive Reactors

Mark E. Byrne[a]; Phillip C. Wankat[a]
[a] SCHOOL OF CHEMICAL ENGINEERING, PURDUE UNIVERSITY, WEST LAFAYETTE, INDIANA, USA

Online publication date: 02 March 2000

To cite this Article Byrne, Mark E. and Wankat, Phillip C.(2000) 'Pressure Effects in Adsorbers and Adsorptive Reactors', Separation Science and Technology, 35: 3, 323 — 351
To link to this Article: DOI: 10.1081/SS-100100160
URL: http://dx.doi.org/10.1081/SS-100100160

SEPARATION SCIENCE AND TECHNOLOGY, **35**(3), pp. 323–351, 2000

Pressure Effects in Adsorbers and Adsorptive Reactors

MARK E. BYRNE and PHILLIP C. WANKAT*
SCHOOL OF CHEMICAL ENGINEERING
PURDUE UNIVERSITY
WEST LAFAYETTE, INDIANA 47907-1283, USA

ABSTRACT

Large transients and oscillations in pressure and flow rate were predicted by an adiabatic equilibrium-staged model when a concentrated strongly adsorbed propane feed was loaded onto zeolite 5A adsorbent initially presaturated with a nonadsorbed component. Oscillations were directly linked to the concentration front of the adsorbable component. When compared to published isothermal results, the adiabatic model produced transients of decreased magnitude in pressure and flow rate, and oscillations were damped. For the adiabatic case, initial breakthrough occurred at slightly earlier times. A parametric study confirmed that a strong finite sink for the adsorbable component and a highly concentrated amount of adsorbable component must be present for oscillations to occur within a staged model. Previous experimental work showed oscillations for columns connected in series with each column behaving as a stage. Adsorbate heat capacity, assumed to be a saturated liquid phase, was shown to be an important energy balance parameter storing approximately 12% of adsorption and compression energy. This term should be included in nonisothermal dynamic models. Kinetic energy and compression effects were determined to be negligible compared to other energy terms. The model was extended to study adiabatic adsorptive reactors. For the reverse water-gas shift reaction, enhanced conversion was confirmed. Pressure transients and oscillations did not occur with strong adsorption since a low concentration of adsorbable species was produced. When the feed contained large amounts of adsorbable component, water, oscillations in pressure and flow rate occurred which produced oscillations in product concentrations and reaction rates. This simulation represents unusual conditions for this reaction, but certainly feasible operating conditions for other reactions. Increasing the reaction equilibrium rate constant,

* To whom correspondence should be addressed. Telephone: (765) 494-0814. FAX: (765) 494-0805. E-mail: wankat@ecn.purdue.edu

which represented new reaction conditions, resulted in a very high conversion with a high purity nonadsorbable product. Enhanced conversion and separation at equivalent energy consumption was confirmed for adsorptive reaction under some but not all conditions.

Key Words. Pressure swing adsorption (PSA); Heat effects; Adsorptive pressure swing reactor (APSR); Pressure swing reactor (PSR); Pressure effects; Adiabatic adsorption; Simulation; Staged model; Adsorptive reaction; Water gas shift reaction

PRESSURE EFFECTS IN ADSORPTION PROCESSES

Since changes in pressure provide the basis for separation in pressure swing adsorption (PSA) processes, pressure effects should be expected to be important in dynamic modeling of these processes. Fluctuations in pressure can be attributed to three areas: pressurization and depressurization, frictional pressure drop through the adsorption bed, and adsorption-caused pressure transients.

Early models of pressurization and depressurization assumed a frozen solid phase (no adsorption or desorption), which assumed that the gas phase changed with pressure according to the chosen gas law equation (24, 26). Essentially, the pressurization and blowdown steps were instantaneous with a square wave step change in column pressure. Since the pressure changes are not instantaneous, pressure–time history equations (27), linear or exponential approximations (27), and instantaneous pressure changes followed by mass transfer at the new constant pressure (9, 27) have been used and provided more realistic solutions.

In most conventional PSA systems, which use large particle diameters and short bed lengths, the frictional pressure drop can be neglected (9). Others include either Darcy's law (Blake–Kozeny equation) or the Ergun equation to account for frictional pressure drop. Many studies provide experimental (6, 16) and theoretical (9, 16, 29) evidence for the importance of including frictional pressure drop effects in the modeling of certain PSA processes. Significant pressure gradients also occur in rapid PSA (RPSA) (1, 27) which is a cyclic gas adsorption process with short cycle times, small particles, and high gas velocities.

Recently, significant adsorption-caused pressure transients were observed by Arumugam and Wankat (5) and Arumugam et al. (3) when a concentrated, strongly adsorbed component was introduced into a column initially presaturated with a weakly adsorbed component. Experiments with columns-in-series exhibited oscillations in pressure and flow rate, which were in qualitative

agreement with an isothermal staged simulation model and partial differential equation simulation model. These findings indicate the need to include variable pressure equations for cases in which a concentrated component is strongly adsorbed. The first goal of this work was to model these systems for adiabatic operation, since most large-scale adsorption processes fall into this regime.

PRESSURE EFFECTS IN ADSORPTIVE REACTORS

The second goal of this work was to develop a novel adiabatic adsorptive pressure swing reactor (APSR) staged model to predict the effects of transients in pressure and temperature on reaction rates, equilibrium, and product concentrations. If significant transients occur, these effects would also need to be included in the design of concentrated adsorptive reactors.

The chromatographic reactor is one of the earliest examples of coupling separation by adsorption with chemical reaction (e.g., Ref. 23). Later examples include pressure swing reactors (PSR) (1, 13, 17) and rapid PSA (RPSR) reactors (2, 18, 31), moving bed processes (11), and simulated moving bed processes (30). The coupling of reaction and adsorption compared to conventional catalytic reactors may: 1) increase conversions and/or improve selectivities; 2) save energy with lower process operating temperatures; and 3) decrease expenses by reducing catalyst deactivation and intensifying the process.

Most of the theoretical models (1, 17, 18, 22, 31, 32) for the PSR or RPSR configurations concentrate on simple case models to reduce the number of operating parameters and decrease solution complexity. The most common limiting assumptions in these models are isothermal operating conditions, negligible axial pressure gradients, and negligible mass transfer resistances. Also, many experimental (14, 31) and theoretical studies (1, 17) introduce feed streams consisting of dilute reactants in inert gas to maintain isothermal conditions and to reduce pressure gradients dramatically. Commercial realization would be operated under more concentrated and nonideal conditions.

Theoretical studies, which included axial pressure drop (2, 22), used pure reactant feed instead of a dilute composition. Axial pressure gradients are also expected to be significant in RPSR processes. Pressure gradients might also play an important role in concentrated adsorptive reactors if adsorption of one or more components is strong. Transients in pressure will not only influence adsorption kinetics and separation capacity but will directly influence reaction rates and product concentrations. Arumugam and Wankat (4) theoretically showed that adsorption-induced pressure gradients and flow rate changes can modify reaction rates and product concentrations in an isothermal gas-phase

adsorptive reactor. This work confirmed the need to include pressure effects in adsorptive reactor modeling when adsorption is strong irrespective of the net change in total moles by reaction (pressure influence on reaction).

Experimental results have confirmed the advantages of PSR systems (8, 13, 31). Recently, the water-gas shift reaction has been of interest (8, 14). Carvill et al. (8) introduced a pure equimolar feed gas of reactants and experimentally confirmed a sorption-enhanced reaction process using a bench-scale apparatus. The reaction considered was the endothermic reverse water-gas shift reaction:

$$CO_{2(g)} + H_{2(g)} \leftrightarrows CO_{(g)} + H_2O_{(g)} \quad (1)$$

The water was adsorbed, driving the reaction to completion. They succeeded in producing an equivalent carbon dioxide to carbon monoxide conversion with 99+% product purity operating at less than half the normal PFR temperature. The comparison, with catalyst only, was 22% purity operating at the same pressure and temperature as the PSR. They operated at near isothermal conditions by transferring the heats of reaction and adsorption through the reactor walls.

Han and Harrison (13) reported on an adsorptive water-gas shift reaction to produce almost pure hydrogen at equivalent conversions of carbon monoxide. Process savings included replacing an expensive shift catalyst with a relatively inexpensive dolomite sorbent, reducing the amount of excess steam sent to the reactor, and eliminating separation equipment as well as heat exchangers between catalyst beds.

MATHEMATICAL MODEL

Staged Model: Columns-in-Series

Figure 1 is a simple schematic of the staged model. The staged model approximates a single adsorption column where stages are mathematical artifacts. However, the staged model also translates to adsorption columns in series where, in effect, each column is a stage. Columns-in-series have been shown to oscillate experimentally (3), and this configuration is common (e.g., simulated moving beds). The cells-in-series numerical discretization method

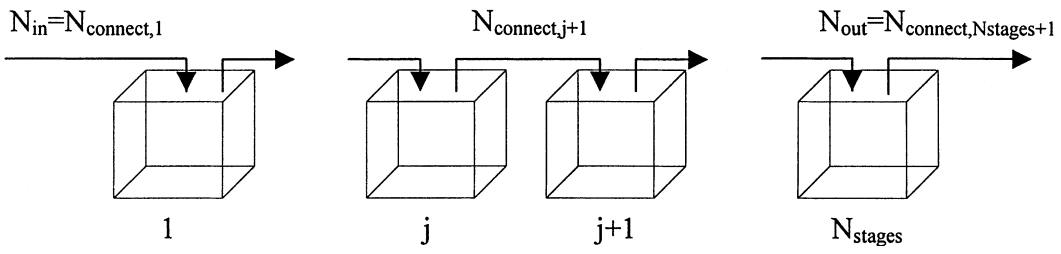

FIG. 1 Schematic for stages-in-series model.

MARCEL DEKKER, INC.
270 Madison Avenue, New York, New York 10016

allows the partial differential equations inherent in modeling column dynamics to be reduced to ordinary differential equations. This numerical approach is equivalent to finite-difference methods (33) and provides adequate computing efficiency. The coupled ordinary differential equations were solved using a dynamic simulation package, SPEEDUP (Aspen Technology, Inc.) (7).

The following assumptions were made in model development: well stirred stages with constant void fraction; negligible radial gradients in temperature, velocity, and concentration; Langmuir adsorption isotherms with Arrhenius temperature dependence; ideal gas behavior; local equilibrium with no mass transfer resistances; instantaneous local thermal equilibrium between fluid and adsorbent; negligible thermal diffusion and pressure diffusion; no viscous heating effects; compressible laminar flow in inlet, outlet, and connecting tubes; no reaction or adsorption in inlet, outlet, and connecting tubes; no energy transfer through column walls; no energy storage in column walls; and mixture properties assumed to be the summation of mole fraction times the pure component properties.

The material balances for the accumulation of total moles in the gas phase in stage j (n_{Tj}) and the moles of component i in stage j in the gas phase (n_{ij}) are

$$\frac{dn_{T,j}}{dt} = N_{\text{connect},j} - N_{\text{connect},j+1} - \rho_p V_j (1-\varepsilon_e)(1-\varepsilon_p) \times \sum_{i=A,B,C,D,I} \left[\frac{dq_{i,j}}{dt}\right] + \sum_{i=A,B,C,D,I} \upsilon_{i,j} R_j \tag{2}$$

$$\frac{dn_{i,j}}{dt} = y_{i,j-1} N_{\text{connect},j} - y_{i,j} N_{\text{connect},j+1} - \rho_p V_j \times (1-\varepsilon_e)(1-\varepsilon_p)\left[\frac{dq_{i,j}}{dt}\right] + \upsilon_{i,j} R_j \tag{3}$$

The gas-phase reverse water-gas shift reaction is equilibrium controlled. It is an equimolar, endothermic reaction that is not thermodynamically favored at temperatures below 800°C (8). The rate of the reverse water-gas shift reaction in stage j is

$$R_j = (\varepsilon_e + (1-\varepsilon_e)\varepsilon_p) V_j \rho_p k_{rj} \left(\frac{1}{K_{pj}} y_{CO_2,j} y_{H_2,j} - y_{H_2O,j} y_{CO,j}\right) \tag{4}$$

The water-gas shift reaction equilibrium constant and reverse rate constant (12) are

$$k_{rj} = (0.86 + 0.14 P_j) \exp\left(1.22 - \frac{1855}{T_j}\right) \quad \text{and} \quad K_{pj} = \exp\left(-4.72 + \frac{4800}{T_j}\right) \tag{5}$$

MARCEL DEKKER, INC.
270 Madison Avenue, New York, New York 10016

where

$$K_{pj} = k_{rj}/k_{fj} \tag{6}$$

The equilibrium constant is the inverse of the normal form since the WGSR is usually written (12) as

$$H_2O + CO \leftrightarrows H_2 + CO_2$$

The reaction constants assume a low temperature shift catalyst with a copper active agent and no deactivation, poisoning, or sintering. It was also assumed that adsorption and reaction take place independently on the adsorbent surface. The heat of reaction must also be evaluated at T_{ref}.

The ideal gas law takes the form

$$P_j = \frac{n_{T,j} R_g T_j}{[\varepsilon_e + (1 - \varepsilon_e)\varepsilon_p] V_j} \qquad \text{and} \qquad y_{i,j} P_j = \frac{n_{i,j} R_g T_j}{[\varepsilon_a + (1 - \varepsilon_e)\varepsilon_p] V_j} \tag{7}$$

With the assumption of compressible laminar flow, the flow rate is (28)

$$N_{connect,j} = \frac{C\pi D^4_{connect,j} \left(P^2(j-1) - P^2(j)\right)}{256\, R_g T \mu_{connect,j} L_{connect,i}} \tag{8}$$

where $P(0) = P_{in}$ and $P_{(N_{stages}+1)} = P_{out}$.

The constant C is introduced to account for flow resistances due to valves, elbows, and so forth. The connecting tubes are hypothetical constructs which have no volume and provide a convenient alternative to account for axial pressure drop within the staged model. No heat transfer, energy storage, viscous heating, or reaction occurs in the connecting tubes.

The amount of component i adsorbed in stage j is given by the Langmuir isotherm,

$$q_{i,j} = \frac{K_{i,j} y_{i,j} P_j}{1 + \sum_{i=A,B,C,D,I} b_{i,j} y_{i,j} P_j} \tag{9}$$

The isotherm parameters are assumed to have an Arrhenius temperature dependence.

$$\frac{b_{i,j}}{b_{0,i}} = \exp\left(\frac{\Delta \hat{H}_{ads,i}}{R_g}\left(\frac{1}{T_0} - \frac{1}{T_j}\right)\right) \qquad K_{i,j} = q_{max,i} b_{i,j} \tag{10}$$

MARCEL DEKKER, INC.
270 Madison Avenue, New York, New York 10016

The energy balance for stage j is

$$\frac{d}{dt}\left[(\varepsilon_e + (1-\varepsilon_e)\varepsilon_p)\hat{H}_j n_{T,j} + (1-\varepsilon_e)(1-\varepsilon_p) \times \hat{H}_{\text{solid},j}\rho_p V_j + (1-\varepsilon_e)(1-\varepsilon_p)V_j\rho_p q_j \hat{H}_{\text{ads},j}\right] = N_{j-1}\hat{H}_{j-1} - N_j\hat{H}_j - \Delta\hat{H}_{\text{rxn}}R_j + \text{KE}_{\text{in}} - \text{KE}_{\text{out}} \quad (11)$$

The first term on the left-hand side of Eq. (11) is the accumulation of energy in the gas inside and outside the porous adsorbent. The second term is the accumulation of energy in the solid within a given stage. The third term is the accumulation of energy in the adsorbate phase.

Differentiating the first term (accumulation of energy in the gas inside and outside the pores) on the left-hand side gives

$$\frac{d}{dt}\left[(\varepsilon_e + (1-\varepsilon_e)\varepsilon_p)\,\hat{H}_j n_{T,j}\right] = (\varepsilon_e + (1-\varepsilon_e)\varepsilon_p) \times \left(C_{\text{pf},j} n_{T,j}\frac{dT_j}{dt} + \hat{H}_j\frac{dn_{T,j}}{dt}\right) \quad (12)$$

where $C_{\text{pf},j}$ $(= d\hat{H}_j/dT_j)$ is the heat capacity of the fluid (gas) phase. The heat capacity of the ideal gas mixture is the weighted average of pure component heat capacities. A polynomial correlation was used for the pure component heat capacities (25):

$$C_{\text{pf},j} = B + 2CT_j + 3DT_j^2 + 4ET_j^3 + 5FT_j^4 \quad (13)$$

The solid and adsorbed phase heat capacities are assumed to have no temperature dependence. The general molar enthalpy for the gas, solid, and adsorbed phases were assumed to be of the form:

$$\hat{H}_j = \int_{T_{\text{ref}}}^{T_j} C_p\, dT \quad (14)$$

The constant of integration is evaluated at $T = T_{\text{ref}}$.

$$\hat{H}_{\text{solid}} = 0, \qquad \hat{H}_{\text{ads}} = \Delta\hat{H}_{\text{ads}}, \qquad \text{and} \qquad \hat{H}_{\text{gas,stage}j} = \hat{H}_j = 0 \qquad \text{at } T = T_{\text{ref}} \quad (15)$$

Therefore, the enthalpy of the solid phase is given by

$$\hat{H}_{\text{solid}j} = \int_{T_{\text{ref}}}^{T_j} C_{\text{psolid}}\, dT \quad (16)$$

where the heat capacity of the solid, $C_{\text{P solid}}$, is a constant independent of temperature and pressure.

These conditions also require the enthalpy of the adsorbed phase to be

$$\hat{H}_{\text{ads}} = \int_{T_{\text{ref}}}^{T_j} C_{\text{pads}}\, dT = C_{\text{pads}}\,(T_j - T_{\text{ref}}) + \Delta\hat{H}_{\text{ads}} \tag{17}$$

where $\Delta\hat{H}_{\text{ads}}$ is the isosteric heat of adsorption at T_{ref}. Most models ignore this contribution of the adsorbate phase. A few other papers have included the adsorbate heat capacity and assumed it to have the properties of a saturated liquid (20, 21). In this modeling effort, C_{pads} was numerically the same as the liquid heat capacity.

Differentiating the second term (accumulation of energy in the solid phase) on the left side gives

$$\frac{d}{dt}\left[(1-\varepsilon_e)(1-\varepsilon_p)\,\hat{H}_{\text{solid},j}\rho_p V_j\right] = (1-\varepsilon_e)(1-\varepsilon_p)\rho_p V_j C_{\text{psolid}}\frac{dT_j}{dt} \tag{18}$$

Differentiating the third term (accumulation of energy in the adsorbate) gives

$$\frac{d}{dt}\left[(1-\varepsilon_e)(1-\varepsilon_p)V_j\rho_p q_j \hat{H}_{\text{ads},j}\right] = (1-\varepsilon_e)(1-\varepsilon_p)\,V_j\rho_p \times \left(\frac{dq_j}{dt}\left(C_{\text{pads}}\,(T_j - T_{\text{ref}}) + \Delta\hat{H}_{\text{ads}}\right) + q_j C_{\text{pads}}\frac{dT_j}{dt}\right) \tag{19}$$

The heat of mixing is assumed to be zero, which is generally a reasonable assumption for gases. For an ideal gas, enthalpy is independent of pressure.

RESULTS

Adsorption: Adiabetic and Isothermal Case Comparison

The simulations modeled an experiment where a column filled with helium at atmospheric pressure is first completely pressurized with helium to a pressure of 3.7228 atm (40 psig) and at $t = 20$ seconds the flow is switched to propane. Results of the adiabatic and isothermal simulations for three stages-in-series are presented in Figs. 2–6. Table 1 lists simulation parameters. The simulation code was slightly modified to achieve isothermal conditions, which matched previous simulation results (3, 5) and qualitatively matched previous experimental results (3). Parametric studies were performed within widely bounded ranges to analyze variable trends even though, in some cases, certain values cannot be achieved with existing technology.

Pressure and Flow Rate Transients

The occurrence of oscillations is linked to the movement of the propane concentration front. A brief description of events is presented here; a full description is presented elsewhere (3, 5, 7). Figures 2 and 3 show oscillations in

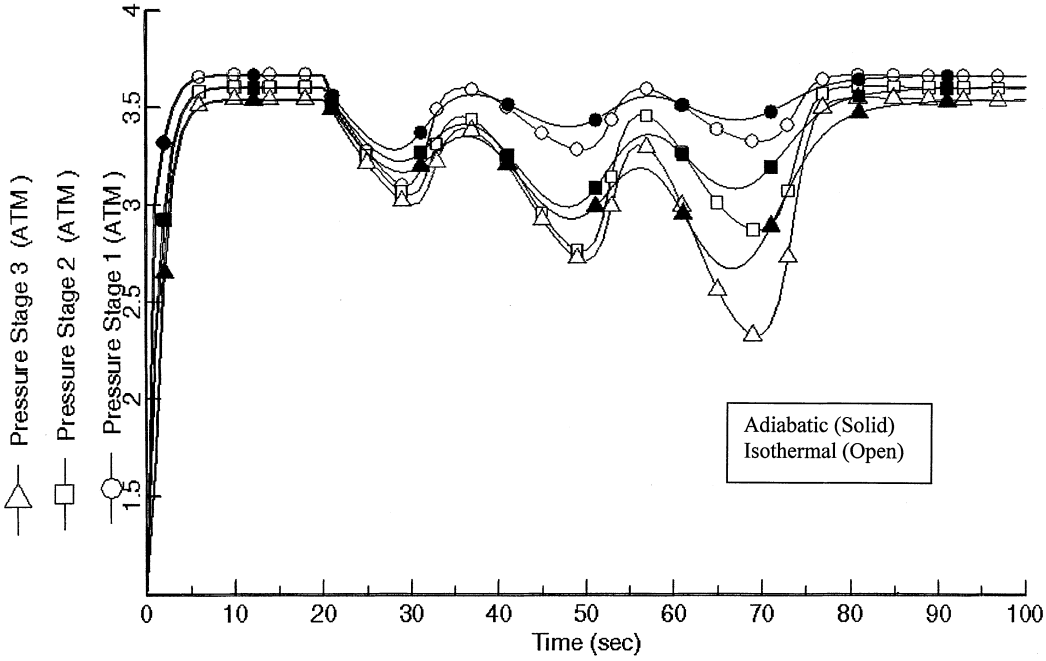

FIG. 2 Three stages-in-series model: Isothermal and adiabatic case comparison—Pressure.

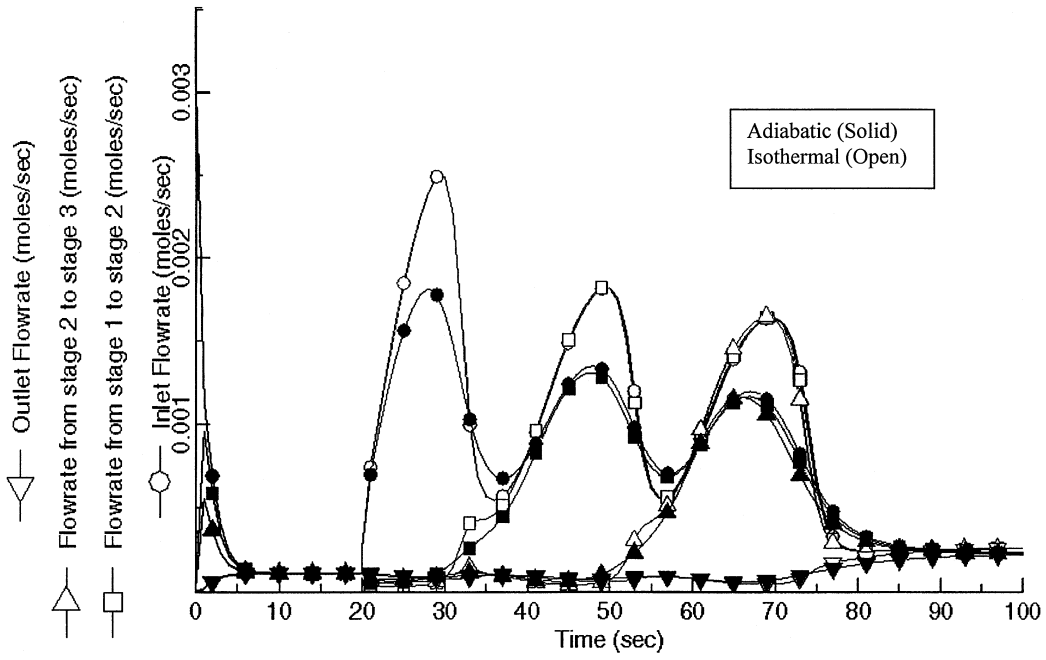

FIG. 3 Three stages-in-series model: Isothermal and adiabatic case comparison—Flow rate.

MARCEL DEKKER, INC.
270 Madison Avenue, New York, New York 10016

TABLE 1
Stages-in-Series Simulation Parameters[a]

Simulation Conditions

Absorption
Initial conditions: P($t = 0$) = 1 atm, $T(t = 0) = 298$ *K*, helium initial
At $t > 0$ s: Pressurization with helium, $P_{in} = 3.7288$ atm, $T_{in} = 298$ *K*, $P_{out} = 1$ atm
At $t = 20$ s: Flow is switched to propane, $P_{in} = 3.7288$ atm, $T_{in} = 298$ *K*, $P_{out} = 1$ atm
Absorption with Reaction
Initial conditions: $P(t = 0) = 1$ atm, $T(t = 0) = 523$ K, helium initial
At $t > 0$ s: Pressurization with helium, $P_{in} = 4.74$ atm, $T_{in} = 523$ *K*, $P_{out} = 1$ atm
At $t = 20$ s: Flow is switched to reactants, $P_{in} = 4.74$ atm, $T_{in} = 523$ *K*, $P_{out} = 1$ atm

Component Characteristics

Parameter	Units	Propane	Helium	CO_2	H_2	H_2O	CO
K_i	mol/(kg·atm)	18.217	0.0	0.0	0.0	84.033	0.0
$b_{o,i}$(3)	atm^{-1}	6.95525	0.0	0.0	0.0	21.874	0.0
μ_i (19)	atm·s	*8.0928* $\times 10^{-11}$	1.9640×10^{-10}	1.48×10^{-10}	8.88×10^{-11}	1.2×10^{-10}	1.8×10^{-11}
MW_i	kg/mol	0.044	0.004	0.044	0.002	0.018	0.028
$q_{max,i}$ (3)	mol/kg	2.6192	0.0	0.0	0.0	3.8417	0.0
$\Delta H_{ads,i}$	J/mol	−28,000 (34)	0.0	0.0	0.0	−75,286 (8)	0.0
$C_{p\ ads,i}$ (19)[b]	J/(mol·K)	104	0.0	0.0	0.0	75.6	0.0

MARCEL DEKKER, INC.
270 Madison Avenue, New York, New York 10016

A_i (25)	J/(mol)	-2.2507×10^{2}	0.0	4.885×10^{2}	5.729×10^{1}	-1.030×10^{2}	-6.347×10^{1}
B_i	J/(mol·K)	5.9538×10^{1}	20.79	2.106×10^{1}	2.677×10^{1}	3.4435×10^{1}	3.004×10^{1}
C_i	J/(mol·K^2)	3.9626×10^{-2}	0.0	3.350×10^{-2}	5.914×10^{-3}	-7.116×10^{3}	-4.8296×10^{-3}
D_i	J/(mol·K^3)	2.6939×10^{-4}	0.0	-1.579×10^{-5}	-7.953×10^{-6}	1.576×10^{-5}	8.4539×10^{-6}
E_i	J/(mol·K^4	-2.4099×10^{-7}	0.0	3.725×10^{-9}	5.318×10^{-9}	-8.903×10^{-9}	-3.847×10^{-9}
F_i	J/(mol·K^5)	6.5845×10^{-11}	0.0	2.539×10^{-13}	-1.219×10^{-12}	1.868×10^{-12}	5.605×10^{-13}

Stages-in-series Model Characteristics

Adsorbent characteristics		Type: 5A zeolite value	STAGE characteristics	
Parameter	Units		Parameter	Value/units
C_p solid (10)	J/(kg·K)	861.6	V^c	1.686×10^{-5}m^3
ρ_p (3)	kg/m^3	1534	ε_e	0.47
ε_p	No units	0.34	L_{in}	0.1 m
Other parameters			$L_{connect}{}^c$	0.1 m
R_g	(m^3·atm)/(mol·K)	8.21×10^{-5}	L_{out}	2.5 m
T_{ref} (reaction value)	K	273 [523]	D, $D_{connect}$	1.75×10^{-3}
ΔH_{rxn} (8)	J/(mol CO)	39,315	C	0.001

[a] Reference citation indicates where parameter value was obtained.
[b] Denotes saturated liquid properties.
[c] Denotes revision to normalize when N_{stages} changes from 3 to 5, or 25.

MARCEL DEKKER, INC. 270 Madison Avenue, New York, New York 10016

pressure and flow rate comparing the isothermal and adiabatic conditions. When flow is switched from helium to propane at $t = 20$ seconds, the amount of propane entering stage 1 is not sufficient to compensate for the propane adsorbed and the total flow out of stage 1. The stage pressure decreases and drops well below the value expected due to purely frictional losses; frictional losses are evident after pressurization (before the propane switch) and after adsorbent saturation. Due to the constant pressure source and since flow rate is proportional to the difference in stage pressure and source pressure, the inlet flow rate to stage 1 (Fig. 3) increases because of the increased pressure drop. Stages 2 and 3 pressures decrease since the flow rate out of stage 1 decreases. When the adsorbent in stage 1 saturates, stage pressure increases and inlet flow rate decreases. The process then repeats for each stage, with one oscillation occurring per stage. Results from simulations for five and 25 stages-in-series (7) confirm as many pressure minima and flow maxima as stages. However, the amplitudes decrease and smooth out as stages increase to approximate a single column. In this regard, oscillations are an artifact of using a staged model to approximate a single column. However, columns-in-series will oscillate (3) with each column acting as a stage. Therefore, these results will be applicable to any staged system.

In comparison to the isothermal case, the pressure and flow rate oscillations of the adiabatic case are broader with decreased amplitude. The pressure minima and flow rate maxima occur at slightly earlier times. Also, total bed saturation is reached at longer times for the adiabatic case. In effect, an additional degree of freedom (temperature not constant) constrains the nature of the response for the adiabatic case. Parametric analysis revealed that pressure and flow transients are a direct consequence of strong adsorption affinity and that oscillations are a result of stages-in-series with a finite adsorption capacity. A single CSTR model (5), which solves a set of similar equations, provided evidence that the oscillations were unlikely to be produced by numerical instability. Experimental evidence also supports this conclusion (3).

Axial pressure and concentration profiles for both cases are presented in Figs. 4 and 5, respectively. Note the discontinuity in the pressure curves at the location of the propane concentration front. For the adiabatic case (Fig. 6), the temperature waves travel slightly ahead of the concentration wave.

Heat Effects

There are three sinks for the energy released by the heat of adsorption: the storage of energy in the adsorbent pellet, the storage of energy in the adsorbed phase (assumed to have the same properties as a liquid), and the storage of energy within the gas inside and outside the pores of the adsorbent. Due to adiabatic conditions, the heat of adsorption and compression energy (parametric evaluation revealed compression energy was insignificant compared to ad-

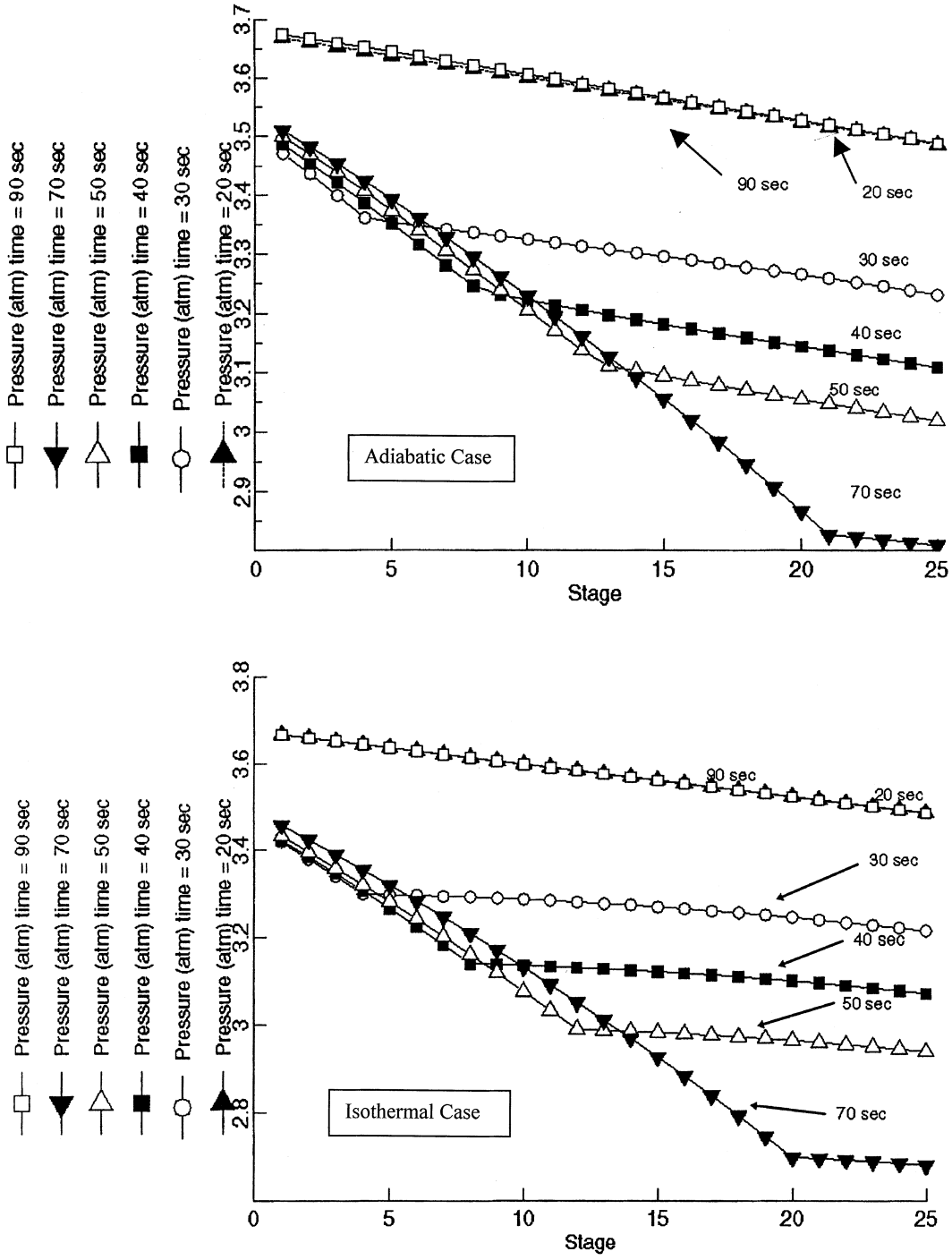

FIG. 4 Twenty-five stages-in-series model: Axial pressure profile.

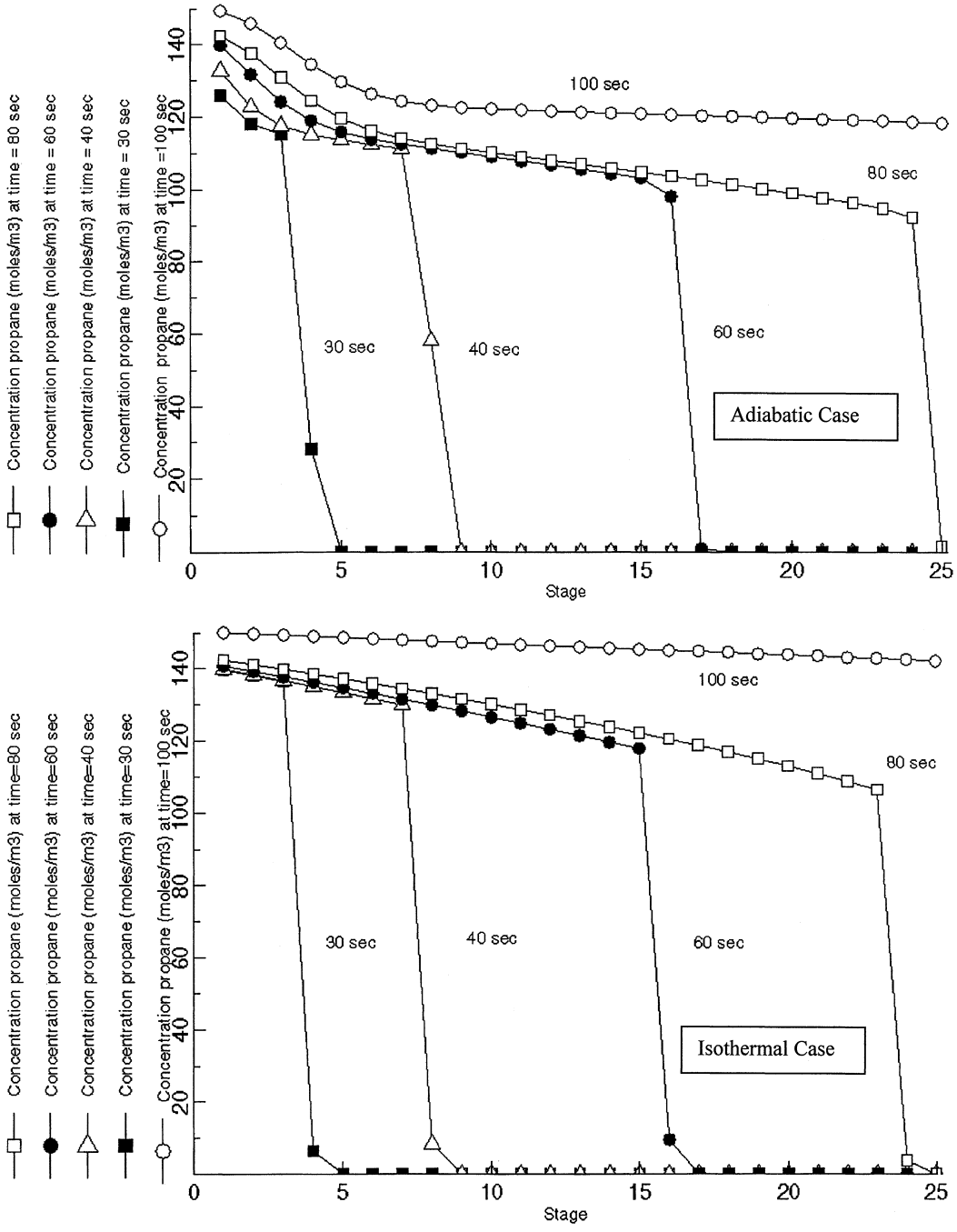

FIG. 5 Twenty-five stages-in-series model: Axial propane concentration profile.

sorption energy) cannot be transferred to the environment into or through stage walls and must be transferred away by the exiting gas.

The heat released by adsorption will raise the temperature within a given stage (Fig. 6). Temperatures of all stages quickly increase and reach higher

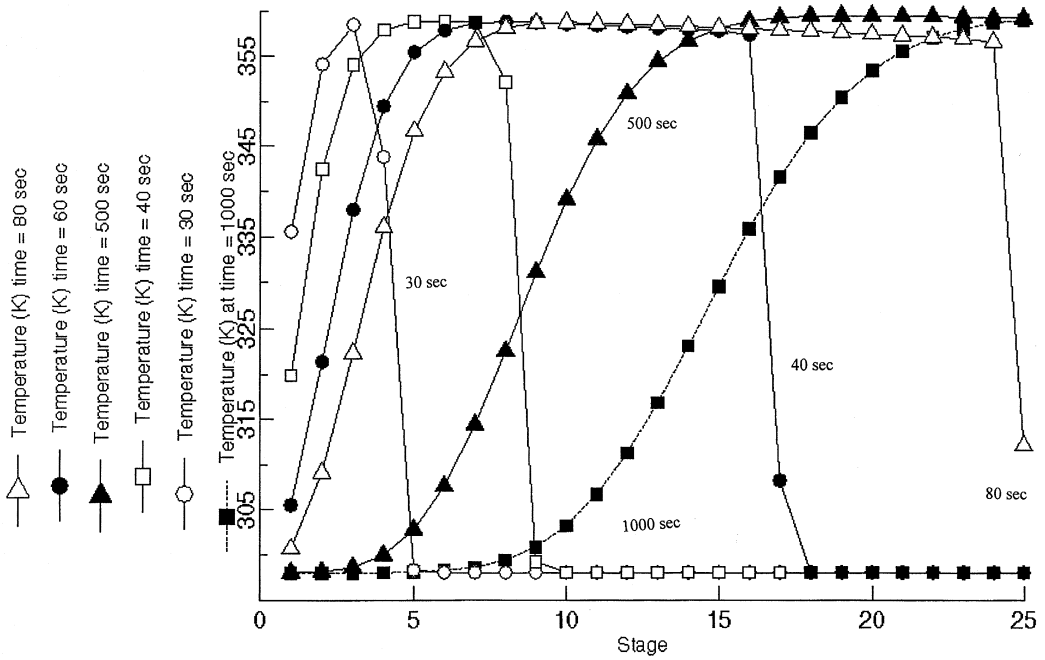

FIG. 6 Twenty-five stages-in-series adiabatic model: Axial temperature profile.

maximums with increasing stage numbers since each stage receives a higher inlet temperature. The combined decrease in pressure from the decrease in the number of gas-phase moles and the increase in temperature from the heat of adsorption decreases propane adsorption. Hence, propane breakthrough occurs earlier for the adiabatic system (Fig. 5). This was verified by analyzing adsorbent loading curves and gas-phase propane curves.

Significant heat effects can decrease the separation efficiency. Temperature changes affect the equilibrium capacity of the adsorbent, the shape of the adsorption isotherm, and adsorption kinetics. The magnitude of the temperature swing depends upon the heat of adsorption, the input concentrations of adsorbable components, cycle time, and the heat transfer characteristics of the column and adsorbent. It is generally accepted that heat effects are detrimental to PSA processes (10, 26, 27, 33) and that adiabatic operation produces the worst performance unless the energy can be used for other purposes, such as regeneration (20, 26, 27).

The main accumulation of energy is within the solid phase (approximately 88%). The energy in the gas phase is negligible compared to the other energy balance terms. Energy is released by the heat of adsorption, which is slightly reduced by the addition of an adsorbate heat capacity (assumed to be saturated liquid heat capacity). This component accumulates approximately 12% of the total energy released. Ignoring this contribution results in approximately 15 K

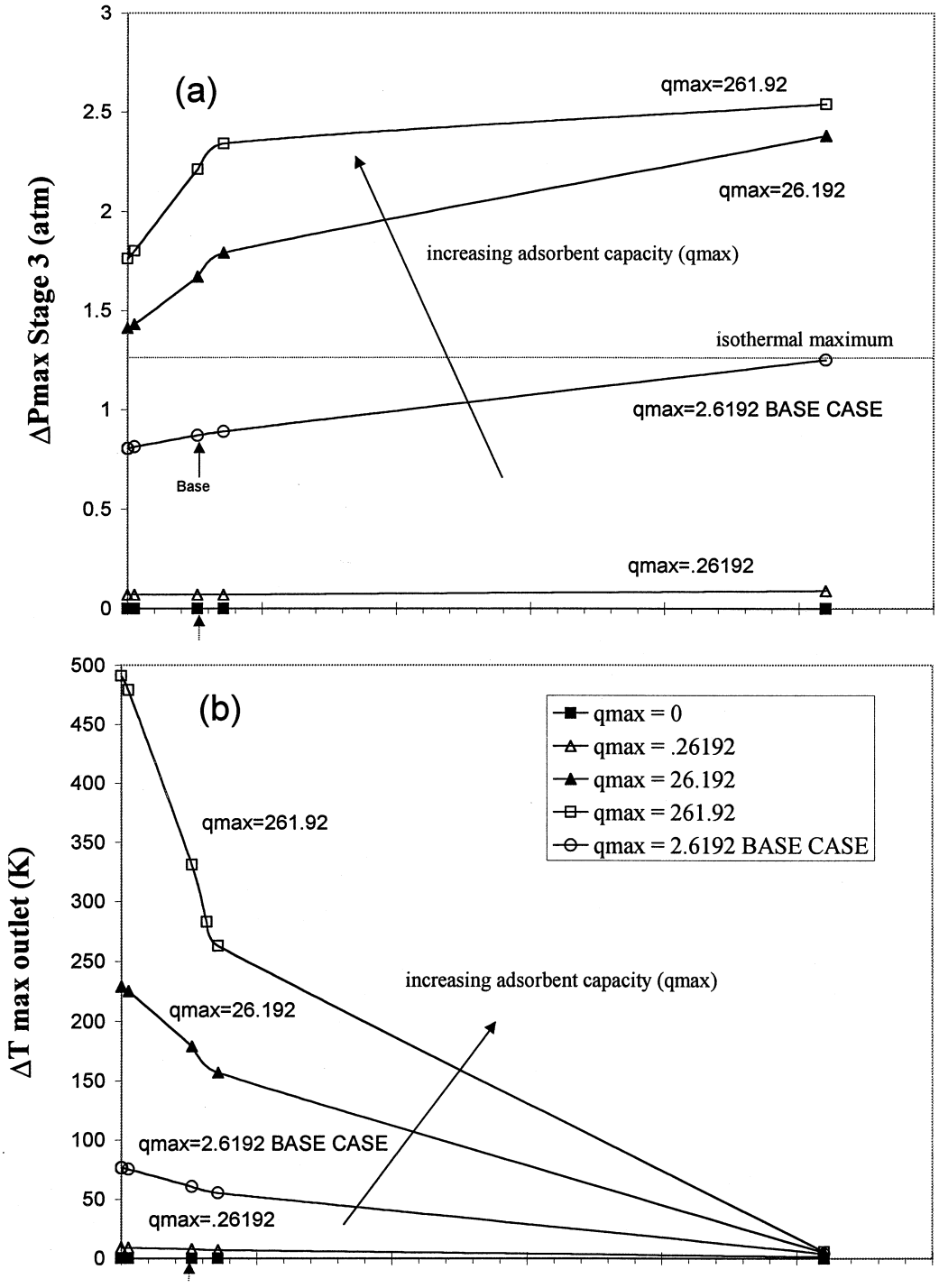

FIG. 7 Three stages-in-series adiabatic model: Adsorbate heat capacity and loading capacity evaluation for 100% propane feed—(a) Maximum pressure difference, (b) Maximum temperature difference, (c) Breakthrough time. Base case/value parameter denotes normal value used in adiabatic base case.

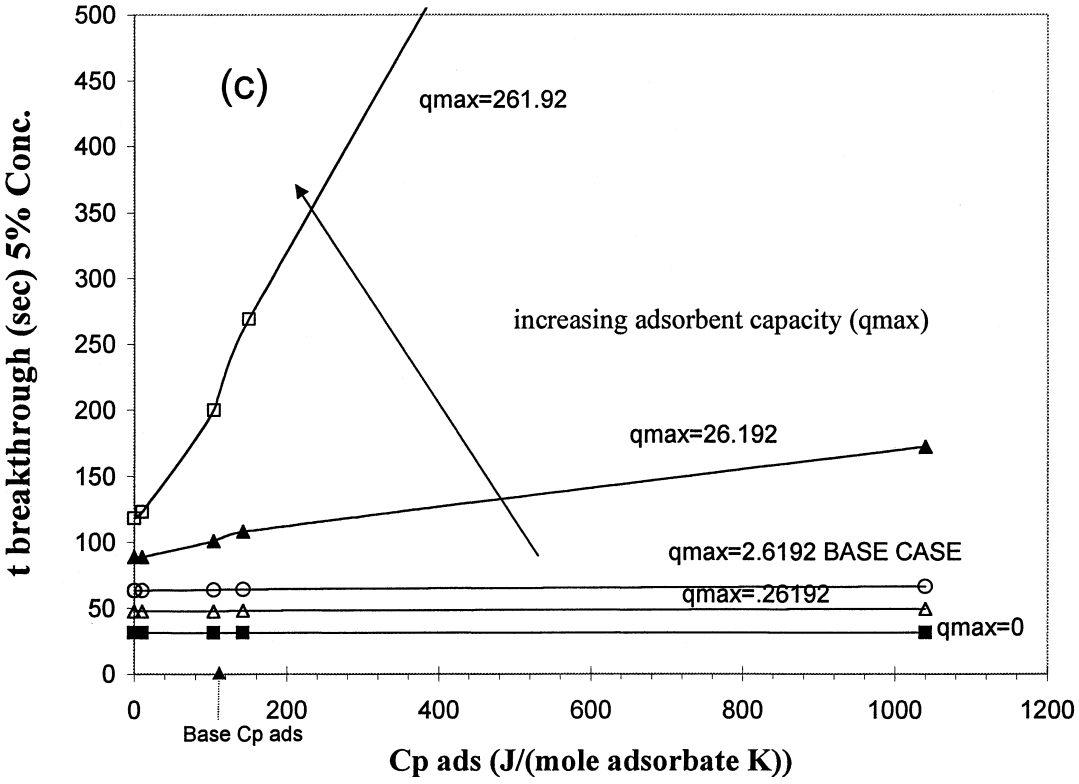

FIG. 7 Continued

overestimation of maximum temperature increase (Fig. 7; compare ΔT_{max} for the base case to the value with $C_{pads} = 0$). Although, since the magnitude of this term depends upon the molar amount of adsorbed component, the effect increases as adsorption occurs. Therefore, this synergistic effect increases this heat sink contribution and is dependent upon adsorption capacity and adsorbed phase heat capacity.

Most papers ignore the contribution of the adsorbed phase heat capacity in the energy balance, and papers (15, 21) that have included it have differed in the nature of the adsorbed phase. Liu and Ritter (20) theoretically analyzed periodic heat effects in PSA and have noted that the inclusion of an adsorbed phase heat capacity (assumed to be saturated liquid) in the model energy balance significantly affected process performance. Of course, when the column approached an isothermal condition by increasing heat transfer to the surroundings, the effects of this term decreased and were no longer noticeable.

Figure 7 shows the combined effects of adsorbent loading capacity and adsorbate heat capacity. For larger values of the heat capacity, isothermal conditions are approached for all cases of loading capacity. For small values, the maximum temperature increases as loading capacity increases. As adsorbent loading capacity is increased, the heat capacity contribution of the adsorbate

will be greater. As more adsorbate is present on the adsorbent, the more energy it can take away as a heat sink. The pressure transients become larger as the adsorbent heat capacity and loading capacity (q_{max}) increase.

The calculations of kinetic energy and enthalpy in and out of each stage proved that the kinetic energy is a small proportion (less than 1%) of the energy in and out of a given stage. Thus, it is a good assumption to neglect kinetic energy contributions with the most influential limiting case presented here, a strongly adsorbed component that produces significant transients in pressure and flow rate.

When the inlet flow rate was held constant, pressure and flow rate transients were of greater magnitude, but the oscillations were reduced. Since the inlet flow rate and the outlet pressure were held constant, the stage pressures reached lower minima.

Inert adsorbent studies produced no pressure or flow transients and confirmed adsorption caused the observed behavior. It also confirmed relatively insignificant heat of compression energy compared to adsorption energy.

Increasing the concentration of presaturant adsorbable component or decreasing the adsorbable component in the feed reduced the adsorbent loading rate, leading to decreased transients and oscillatory behavior. Temperature swings were also reduced. Parametric analysis for the propane/helium system revealed that 80% propane was the lowest feed concentration that produced significant transient/oscillatory behavior (approximately 0.2 atm pressure transient).

As the adsorbent and adsorbate heat capacities were increased, isothermal operation was approached; the outlet temperature maxima decreased, pressure minima decreased (amplitude increase), and breakthrough time increased.

Increasing adsorbent capacity q_{max} resulted in higher temperature swings and larger pressure transients (larger than isothermal case). However, large factors greater than an order of magnitude produced an overall pressure depression which replaced oscillations. Thus, as the finite capacity restriction on the sink was removed, oscillations were no longer present. The effects of changing both adsorbent heat capacity and loading capacity for a pure propane feed are presented in Fig. 8. By increasing the adsorbent heat capacity, more loading (hence separation) can be reached for equivalent temperature fluctuations. For a larger heat capacity, pressure transients are increased for a given loading capacity.

Adsorption and Reaction: Water-Gas Shift Reaction

A column filled with helium at atmospheric pressure is first completely pressurized with helium to a pressure of 4.74 atm (55 psig) and at $t = 20$ seconds the flow is switched to an equimolar feed mixture of reactants, 50% carbon dioxide and 50% hydrogen (adiabatic WGSR base case simulation).

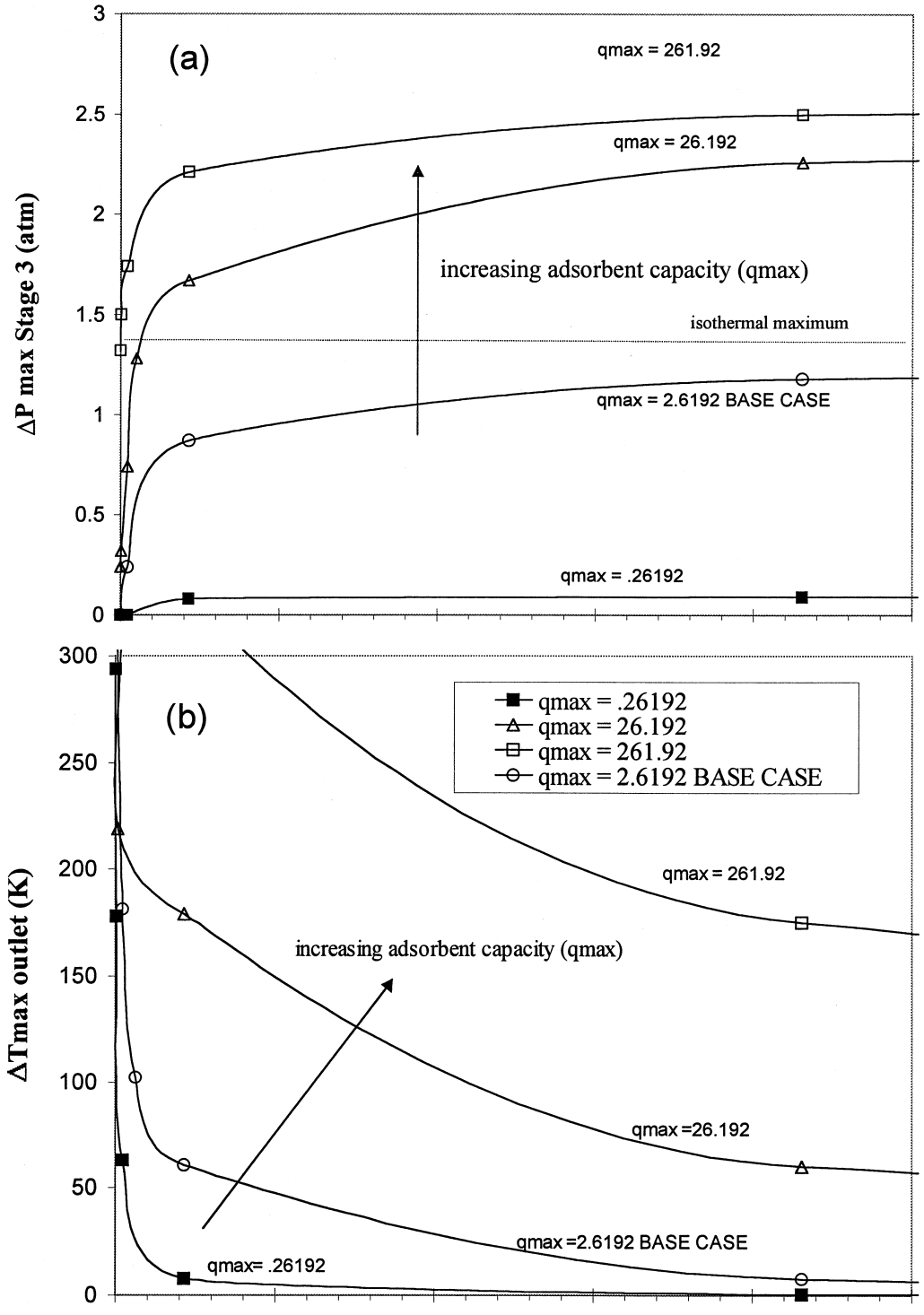

FIG. 8 Three stages-in-series adiabatic model: Adsorbent heat capacity and loading capacity evaluation for 100% propane feed—(a) Maximum pressure difference, (b) Maximum temperature difference, (c) Breakthrough time. Base case/value parameter denotes normal value used in adiabatic base case.

(*continued*)

MARCEL DEKKER, INC.
270 Madison Avenue, New York, New York 10016

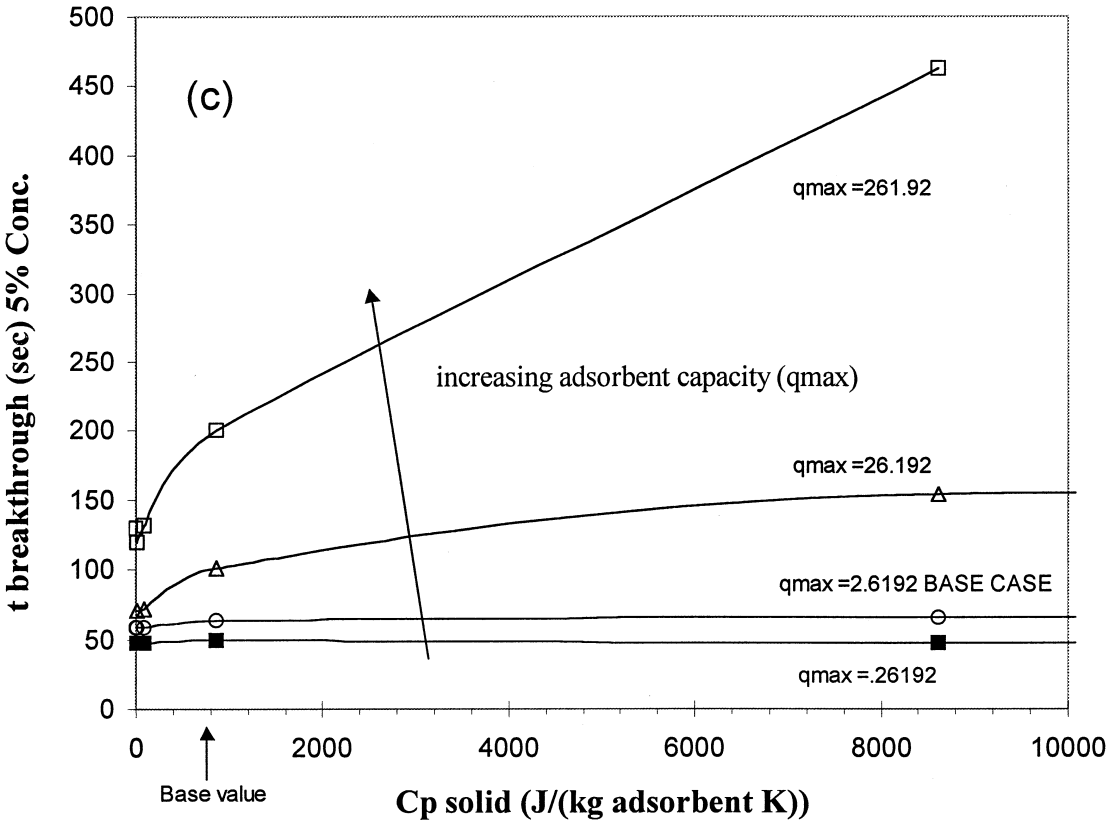

FIG. 8 Continued

Even though a large sink for water (the adsorbable component) existed, the adsorbable component was not concentrated enough to significantly affect the pressure behavior (the maximum mole fraction water can reach is 0.5) and no transient period existed. For a three-stage simulation, stages 1, 2, and 3 temperatures reached maximums of 558, 580, and 590 K, respectively, which were qualitatively similar to adsorption only results. Since the heat of adsorption was larger than the heat needed for reaction, the temperature in stage 1 quickly increased as the equimolar feed entered the stage. Stages 2 and 3 reached higher maximum temperatures than stage 1 because each received a higher temperature gas from the previous stage. A parametric analysis revealed that for endothermic reactions, temperature swings were minimized as the ratio of heat of adsorption/heat of reaction approached unity.

The stage 1 net rate of formation reached a maximum and then decreased since water began to be consumed by the backward reaction, as well as still being adsorbed. Stage 1 reached a higher net rate maximum than stages 2 and 3 due to the larger amounts of carbon dioxide and hydrogen present in the gas phase. As more water was present in the gas phase, the backreaction had a

greater effect until steady-state. When the adsorbent was saturated, both temperature and net rate of formation followed the same trend. As the adsorbent saturated, the mole fraction of water increased. This caused carbon dioxide and hydrogen outlet concentrations to increase and the outlet concentration of carbon monoxide to decrease due to the backreaction until steady-state was reached. The water mole fraction showed a maximum, then decreased due to backreaction.

For similar reaction conditions with no adsorption, all stage temperatures decrease as expected due to the endothermic nature of the reaction. As expected, steady-state results matched the reaction with the adsorption case (when adsorbent is saturated). This was also confirmed by rate of formation curves.

The reaction/adsorption maximum rates of formation are also much higher than the reaction alone case. Reaction with no adsorption produced a maximum outlet concentration of 5 mol/m^3 of carbon monoxide. The reaction/adsorption base case produced a maximum of 20 mol/m^3 of carbon monoxide (steady-state reduces concentration to 5 mol/m^3). Equivalent conversions (20 mol/m^3) with reaction only (no adsorption) were produced by operating at a significantly elevated temperature of 850 K. Thus, enhanced conversion at equivalent energy consumption or equivalent conversion with energy savings is confirmed for APSR.

In order to study transient pressure effects, a 90% water/10% carbon dioxide feed was introduced into stage 1 of a three-stage system. Pressure oscillations (Fig. 9a) occurred with these feed conditions (unusual for this reaction but not for other reactions), and the nature of the transients and oscillations are qualitatively similar to adsorption only results. Since the reaction is exothermic in this direction, the maximum temperature (Fig. 9b) reached by each stage is greater than the equimolar feed WGSR results. This is expected with the superposition of the heats of adsorption and reaction. Rate of formation curves confirmed a high net rate of reaction in stage 1, which is always in the backward direction. However, the net rate of reaction within stages 2 and 3 goes in the opposite direction. This is due to the adsorption and reaction sinks for water. There is also a very high rate of adsorption at early times since water is present in the feed. When breakthrough occurs from stage 1 at approximately $t = 80$ seconds (Fig. 9c), the net maximum rate of formation of water decreases. With water present, the reaction can proceed in the opposite direction. The peaks in net rate of formation correspond to the gas-phase mole fraction of the adsorbable component in the feed, water. Therefore, oscillations in reaction rates are a direct consequence of a highly concentrated, strongly adsorbed component in the feed. The outlet concentrations (Fig. 10) show slight oscillations in product concentrations and reactant, carbon monoxide. As the adsorbent is saturated, outlet water concentration rises slightly and carbon

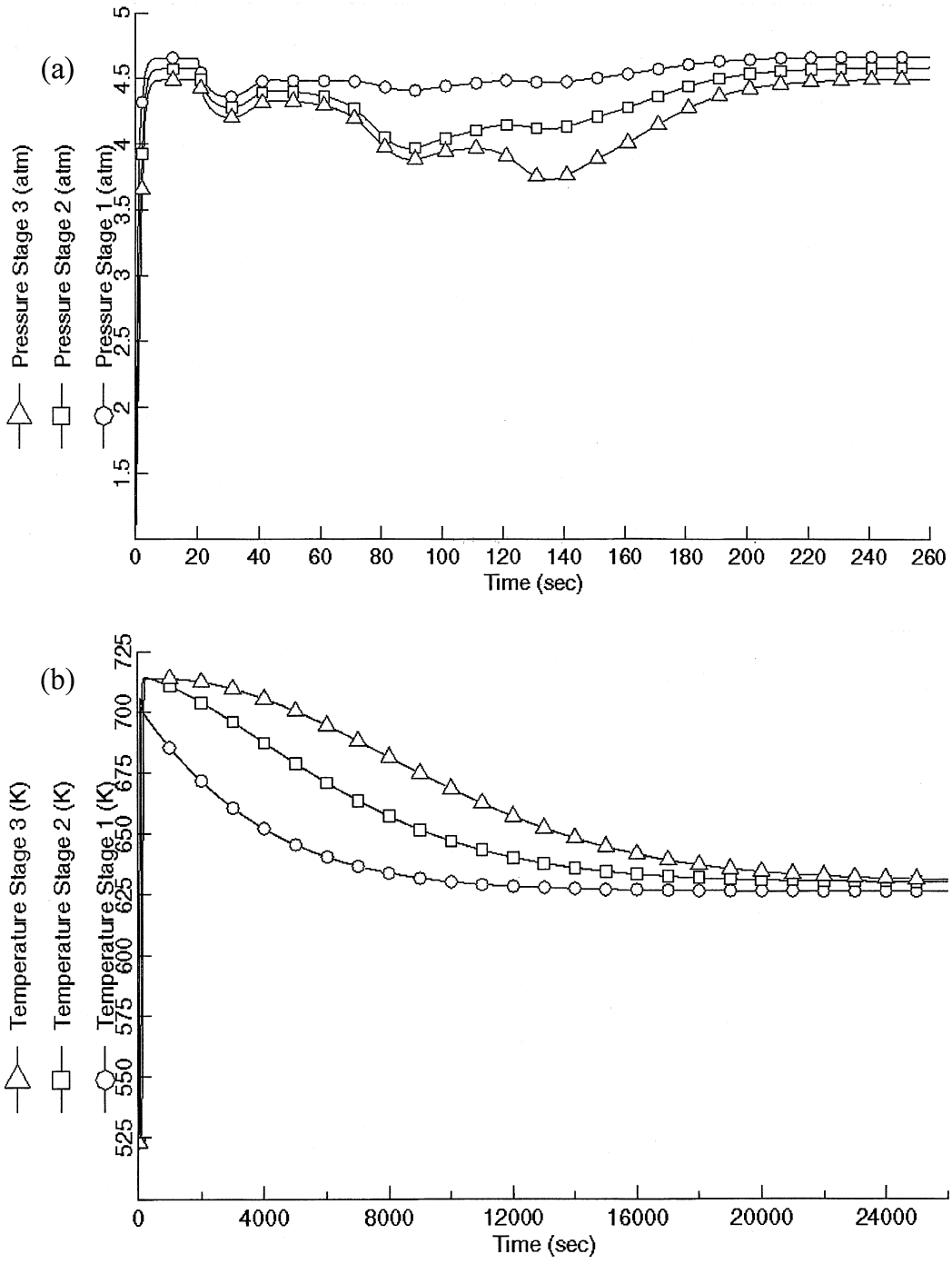

FIG. 9 Three stages-in-series WGSR adiabatic model: 90% H_2O/10% CO feed—(a) Pressure, (b) Temperature, (c) Water breakthrough curves.

MARCEL DEKKER, INC.
270 Madison Avenue, New York, New York 10016

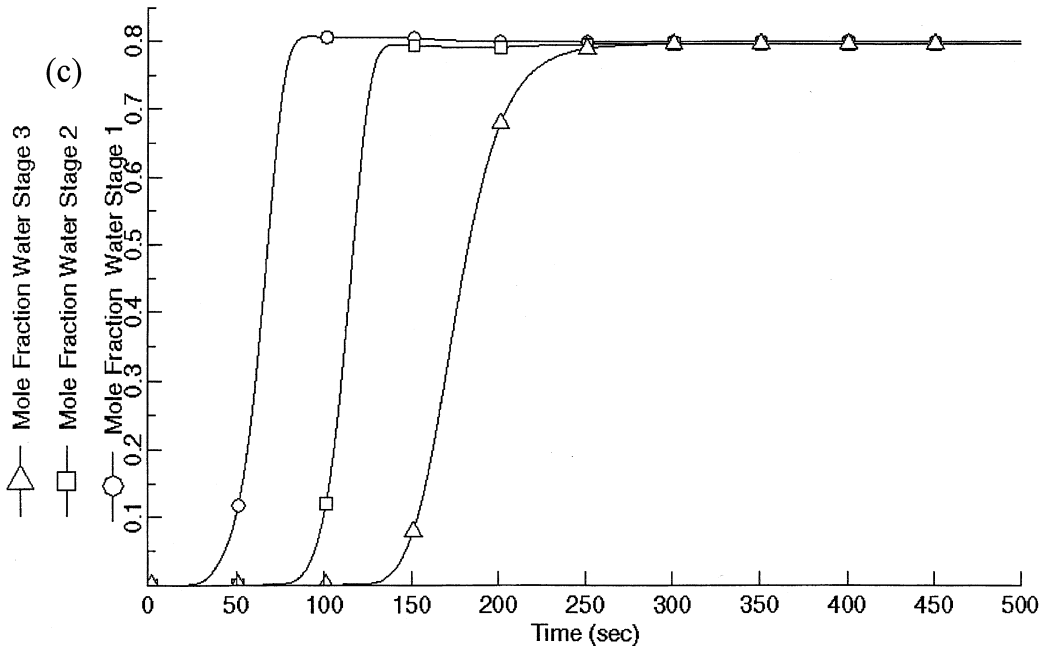

FIG. 9 Continued

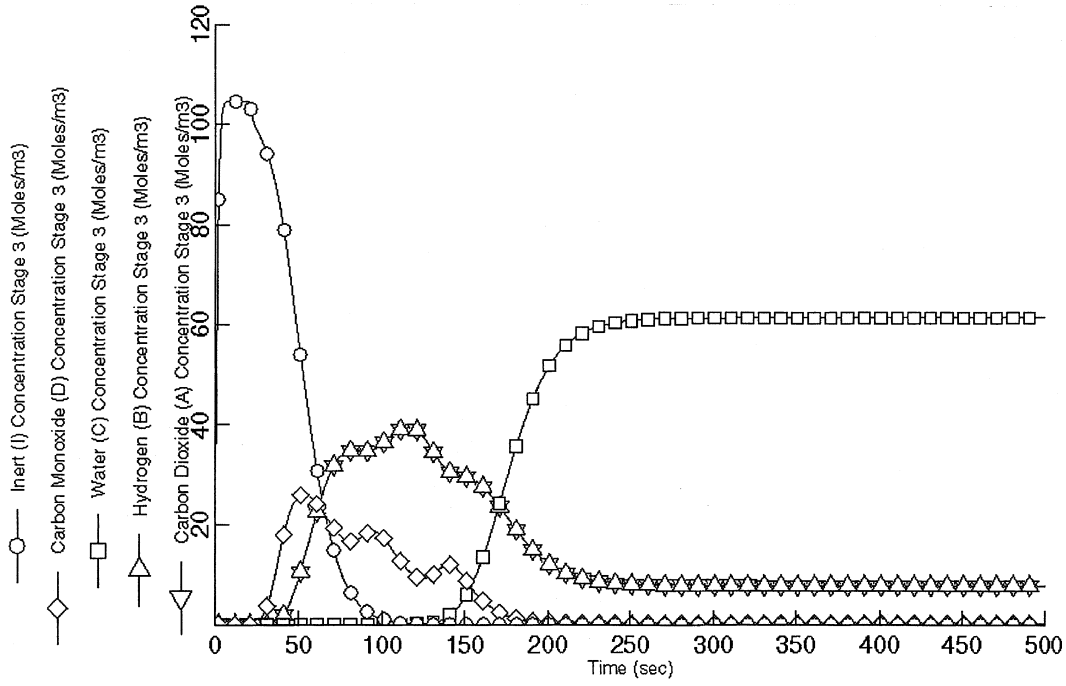

FIG. 10 Three stages-in-series WGSR adiabatic model: 90% H_2O/10% CO feed—Outlet concentration.

MARCEL DEKKER, INC.
270 Madison Avenue, New York, New York 10016

dioxide and hydrogen concentrations are relatively constant since water is reacting (very small backreaction) to form carbon dioxide and hydrogen.

A feed of 50% water/50% carbon monoxide did not produce significant transients or oscillations in pressure or flow rate. No significantly noticeable oscillations occurred in outlet concentrations or in net reaction rates.

As a check, pure water (adsorption only) was fed to the system. Oscillations in pressure were very similar to previous propane adsorption results. The temperature maxima and pressure transients were larger due to stronger adsorption of water and a higher energy of adsorption released.

For three stages, the equilibrium rate constant was arbitrarily increased by a factor of 1000. All other parameters were kept the same as the adiabatic WGSR base case. Slight transients in pressure occurred, but there were no noticeable oscillations. At these conditions it was possible to produce approximately 103 mol/m^3 of CO. Between approximately $t = 100$ to 600 seconds it was also possible to produce an essentially pure product CO. The outlet concentration results are shown in Fig. 11.

Theoretical reactions with a small net decrease or net increase in the number of moles were also simulated with the stages-in-series model (7). Enhanced conversion was confirmed when a strong adsorption sink was present, and oscillations in product concentrations and reaction rates occurred which

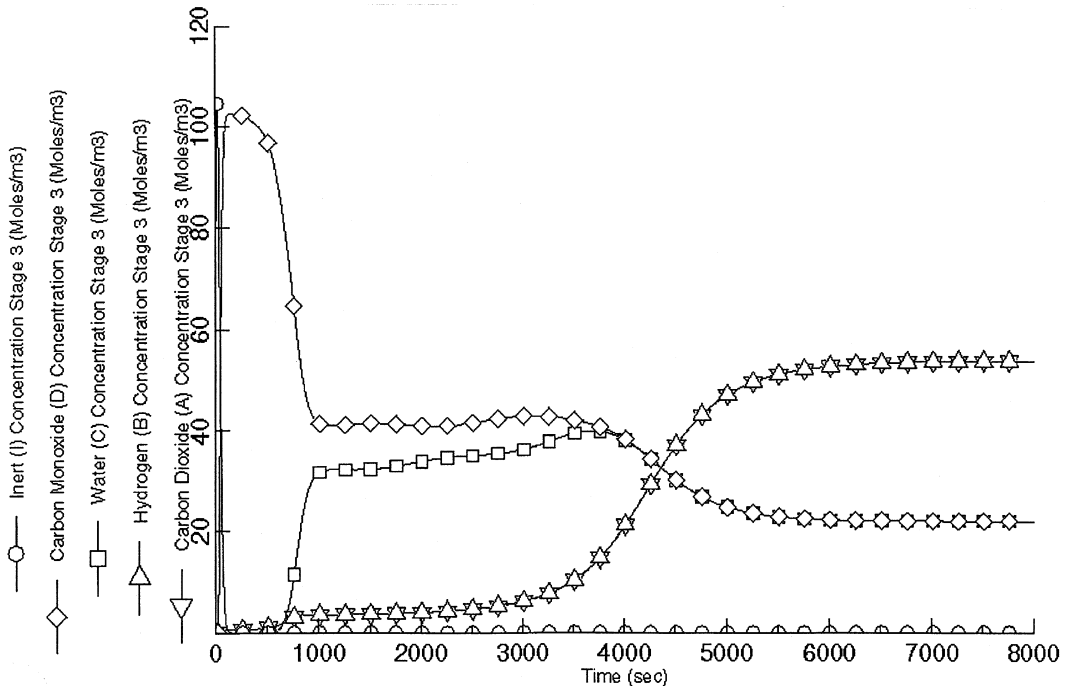

FIG. 11 Three stages-in-series WGSR adiabatic model: Increase in equilibrium reaction constant × 1000—Outlet concentration.

MARCEL DEKKER, INC.
270 Madison Avenue, New York, New York 10016

enhanced or hindered product formation, depending on the volume change by reaction. If both equilibrium reaction rate constant (net formation of adsorbable component) and adsorption capacity are sufficiently large, oscillations will occur. If the exothermic heat of reaction is relatively large, adsorption capacity will be compromised and adsorption-caused effects will not occur. It was confirmed that the APSR increased conversion with all reactions considered, but they are better suited for endothermic reactions with an increase in the number of moles.

CONCLUSIONS

Adsorption without Reaction

Large transients and oscillations in pressure and flow were confirmed to exist when a concentrated strongly adsorbed feed was loaded onto a staged column initially presaturated with a nonadsorbed component. Oscillations were directly linked to the concentration front of the adsorbable component. When compared to isothermal results, an adiabatic model produced transients of decreased magnitude in pressure and flow rate, and oscillations were broader with decreased amplitude. Pressure oscillation minima, flow rate oscillation maxima, and initial breakthrough occurred at slightly earlier times, and steady-state was reached at slightly longer times for the adiabatic case. The most limiting assumption in model development was neglecting mass and heat transfer resistances by assuming equilibrium stages. More importantly, however, the assumption of constant column pressure during feed steps was shown not to be valid when dealing with a concentrated strongly adsorbing system.

Results of a parametric study confirmed that a strong finite sink for the adsorbable component and a highly concentrated amount of the adsorbable component must be present for oscillations to occur in a staged model. The nature of the transients is also dependent upon the amount and rate of energy produced and taken away, and operation can be altered with different energy storage parameters. In particular, adsorbate heat capacity was shown to be an important energy balance parameter that should be included in nonisothermal models. Correct parameter estimation and evaluation in models of these processes is very important in adequately describing behavior.

Adsorption with Reaction

For endothermic reactions with no net change in the number of moles, conversion and separation can be enhanced within an adsorptive reactor. For the adiabatic reverse WGSR, pressure transients and oscillations did not occur with strong adsorption since a low concentration of adsorbable species was produced. However, when the feed was switched to unusual feed conditions

with a large amount of adsorbable component, oscillations in pressure and flow rate occurred which produced oscillations in product concentrations and rates of formation. The oscillations are a direct result of strong adsorption of a highly concentrated component within a staged model. Increasing the equilibrium rate constant resulted in a very high conversion with a period of approximately pure nonadsorbable product.

NOMENCLATURE

A	gas-phase heat capacity polynomial equation coefficient (J/mol)
B	gas-phase heat capacity polynomial equation coefficient (J/(mol·K))
b	equilibrium parameter in Langmuir isotherm expression (atm^{-1})
b_0	equilibrium parameter at temperature T_0 in Langmuir isotherm expression (atm^{-1})
C	1. constant in Eq. (8) to account for flow resistances 2. heat capacity polynomial equation constant (J/(mol·K^2))
C_{pads}	adsorbate phase heat capacity (J/(mol adsorbate·K))
C_{pf}	gas-phase heat capacity (J/(mol·K))
C_{psolid}	solid adsorbent heat capacity (J/(kg adsorbent·K))
D	1. tube diameter (m) 2. heat capacity equation constant (J/(mol·K^3))
E	heat capacity polynomial equation constant (J/(mol·K^4))
F	heat capacity polynomial equation constant (J/(mol·K^5))
$\hat{H}$	molar enthalpy of gas phase (J/(mol·K))
$\hat{H}_{ads}$	molar enthalpy of adsorbate phase (J/(mol adsorbate))
$\hat{H}_{solid}$	enthalpy of adsorbent particle (J/(kg adsorbent))
$\hat{H}_{rxn}$	molar enthalpy of reaction (J/mol)
$\Delta\hat{H}_{ads}$	molar isosteric heat of adsorption (J/(mol adsorbate))
$\Delta\hat{H}_{rxn}$	molar heat of reaction (J/mol)
K	parameter in Langmuir isotherm expression (mol/(kg·atm))
K_p	reaction equilibrium constant; WGSR (no units)
k_f	forward reaction rate constant; WGSR (mol/(kg·s))
k_r	reverse reaction rate constant; WGSR (mol/(kg·s))
KE	kinetic energy (J/s)
L	tube length (m)
MW	molecular weight (kg/gmol)
n	moles in gas phase (mol)
N_{in}, N_{out}	molar flow rate in inlet and outlet tubes (mol/s)
$N_{connect}$	molar flow rate in connecting tubes (mol/s)
P	pressure (atm)

q	adsorbent loading (mol/(kg adsorbent))
R_g	gas constant ($(m^3 \cdot atm)/(mol \cdot K)$)
R	rate of reaction (mol/s)
T	temperature (K)
t	time (s)
V	volume of stage (m^3)
y	mole fraction in gas phase

Greek Letters

ρ_p	adsorbent particle density (kg/m^3)
υ	stoichiometric coefficient
μ	viscosity of gas phase (atm·s)
ε_e	interstitial void fraction
ε_p	intraparticle void fraction
Δ	change

Subscripts

1	refers to stage number 1
A	1. helium in adsorption studies 2. carbon dioxide in water-gas shift reaction
ads	refers to adsorbate characteristics
B	hydrogen in water-gas shift reaction
C	1. propane in adsorption studies 2. water in the water-gas shift reaction
connect	refers to connecting tubes in stages-in-series model
D	carbon monoxide in water-gas shift reaction
I	inert component (helium)
i	refers to component A, B, C, D, or I
in	inlet
j	refers to stage number
$j-1, j+1$	refers to stage preceding stage j, and after stage j
max	refers to maximum loading (adsorbent maximum capacity)
mix	mixing
N_{stages}	total number of stages
$N_{stages+1}$	outlet of last stage
0	refers to reference state
out	outlet
p	refers to adsorbent particle characteristics
ref	refers to reference state
rxn	refers to reaction characteristics
solid	refers to solid (adsorbent) characteristics
T	refers to total

MARCEL DEKKER, INC.
270 Madison Avenue, New York, New York 10016

ACKNOWLEDGMENTS

The authors gratefully acknowledge partial financial support from the National Science Foundation under Grant CTS-9401935.

REFERENCES

1. E. Alpay, D. Chatsiriwech, L. S. Kershenbaum, C. P. Hall, and N. F. Kirkby, "Combined Reaction and Separation in Pressure Swing Processes," *Chem. Eng. Sci.*, *49*(24B), 5845–5864 (1994).
2. E. Alpay, C. N. Kenney, and D. M. Scott, "Simulation of Rapid Pressure Swing Adsorption and Reaction Processes," *Ibid.*, *48*(18), 3173–3186 (1993).
3. B. K. Arumugam, J. F. Banks, and P. C. Wankat, "Pressure Effects in Adsorption Systems," *Adsorption*, *5*, 261–278 (1999).
4. B. K. Arumugam and P. C. Wankat, "Pressure Transients in Gas Phase Adsorptive Reactors," *Ibid.*, *4*, 345–354 (1998).
5. B. K. Arumugam and P. C. Wankat, "Pressure Behavior during the Loading of Adsorption Systems," in *Proceedings of the Fifth International Conference on Fundamentals of Adsorption*, Pacific Grove, California, May 1995, Kluwer Academic Publishers, Boston, MA, 1996, pp. 51–58.
6. M. A. Buzanowski, R. T. Yang, and O. W. Haas, "Direct Observation of the Effects of the Bed Pressure Drop on Adsorption and Desorption Dynamics," *Chem. Eng. Sci.*, *44*, 2392–2394 (1989).
7. M. E. Byrne, "Pressure Effects in Adiabatic Adsorption and Adsorptive Reactors," Master's Thesis, Purdue University, 1997.
8. B. T. Carvill, J. R. Hufton, M. Anand, and S. Sircar, "Sorption-Enhanced Reaction Processes," *AIChE J.*, *42*(10), 2765–2772 (1996).
9. S. J. Doong and R. T. Yang, "The Role of Pressure Drop in Pressure Swing Adsorption," *AIChE Symp. Ser.*, *264*(84), 145–154 (1988).
10. S. Farooq, M. M. Hassan, and D. M. Ruthven, "Heat Effects in Pressure Swing Adsorption Systems," *Chem. Eng. Sci.*, *43*(5), 1017–1031 (1988).
11. B. B. Fish and R. W. Carr, "An Experimental Study of the Counter-Current Moving Bed Chromatographic Reactor," *Ibid.*, *44*(9), 1773–1783 (1989).
12. J. R. Gonzalez-Velasco, M. A. Gutierrez-Ortiz, J. A. Gonzalez-Marcos, N. Amadeo, M. A. Laborde, and M. Paz, "Optimal Inlet Temperature Trajectories for Adiabatic Packed Reactors with Catalyst Decay," *Ibid.*, *47*(6), 1495–1501 (1992).
13. C. Han and D. P. Harrison, "Multicycle Performance of a Single-Step Process for H_2 Production," *Sep. Sci. Technol. 32*(1–4), 681–697 (1997).
14. C. Han and D. P. Harrison, "Simultaneous Shift Reaction and Carbon Dioxide Separation for the Direct Production of Hydrogen," *Chem. Eng. Sci.*, *49*(24B), 5875–5883 (1994).
15. A. Kapoor and R. T. Yang, "Separation of Hydrogen-Lean Mixtures for a High-Purity Hydrogen by Vacuum Swing Adsorption," *Sep. Sci. Technol.*, *23*, 153–178 (1988).
16. E. S. Kikkinides and R. T. Yang, "Effects of Bed Pressure Drop on Isothermal and Adiabatic Adsorber Dynamics," *Chem. Eng. Sci.*, *48*, 1545–1555 (1993).
17. N. F. Kirkby and J. E. P. Morgan, "A Theoretical Investigation of Pressure Swing Reaction," *Trans. Inst. Chem. Eng.*, *72A*, 541–550 (1994).
18. I-D. Lee and R. H. Kadlec, "Effects of Adsorbent and Catalyst Distribution in Pressure Swing Reactors," *AIChE Symp. Ser.*, *84*(264), 167–176 (1988).
19. P. E. Liley, R. C. Reid, and E. Buck, "Physical and Chemical Data," in *Perry's Chemical Engineers Handbook*, Section 3, 6th ed., McGraw-Hill, New York, NY, 1984.

20. Y. Liu and J. A. Ritter, "Periodic State Heat Effects in Pressure Swing Adsorption—Solvent Vapor Recovery," *Adsorption*, *4*(2), 159–172 (1998).
21. Y. Liu and J. A. Ritter, "Evaluation of Model Approximation in Simulating Pressure Swing Adsorption Solvent Vapor Recovery," *Ind. Eng. Chem. Res.*, *35*(7), 2299–2312 (1997).
22. Z. P. Lu and A. E. Rodrigues, "Pressure Swing Adsorptive Reactors: Simulation of Three-Step One Bed Process," *AIChE J.*, *40*(7), 1118–1137 (1994).
23. E. M. Magee, "The Course of a Reaction in a Chromatographic Column," *Ind. Eng. Chem. Fundam.*, *2*, 32–36 (1963).
24. J. E. Mitchell and L. H. Shendalman, "Study of Heatless Adsorption in the Model System CO_2 in He, Part II," *AIChE Symp. Ser.*, *69*(134), 25–32 (1973).
25. C. A. Passut and R. P. Danner, "Correlation of Ideal Gas Enthalpy, Heat Capacity, and Entropy," *Ind. Eng. Chem., Process Des. Dev.*, *11*(4), 543–546 (1972).
26. D. M. Ruthven, *Principles of Adsorption and Adsorption Processes*, Wiley, New York, NY, 1984.
27. D. M. Ruthven, S. Farooq, and K. S. Knaebel, *Pressure Swing Adsorption*, VCH Publishers, New York, NY, 1994.
28. B. C. Sakiadis, "Fluid and Particle Mechanics," in *Perry's Chemical Engineering Handbook*, 6th ed., McGraw-Hill, New York, NY, 1984, p. 5-29.
29. N. Sundaram and P. C. Wankat, "Pressure Drop Effects in the Pressurization and Blowdown Steps of Pressure Swing Adsorption," *Chem. Eng. Sci.*, *43*(1), 123–129 (1988).
30. A. Tonkovich and R. W. Carr, "A Simulated Counter-Current Moving Bed Chromatographic Reactor for the Oxidative Coupling of Methane: Experimental Results," *Ibid.*, *49*(24A), 4647–4656 (1994).
31. G. G. Vaporciyan and R. H. Kadlec, "Periodic Separating Reactors: Experiments and Theory," *AIChE J.*, *35*(5), 831–844 (1989).
32. G. G. Vaporciyan and R. H. Kadlec, "Equilibrium-Limited Periodic Separation Reactors," *Ibid.*, *33*, 1334–1343 (1987).
33. R. T. Yang, *Gas Separation by Adsorption Processes*, Butterworths, Stoneham, MA, 1987.
34. D. M. Young and A. D. Crowell, *Physical Adsorption of Gases*, Butterworths, London, 1962.

Received by editor January 29, 1999
Revision received June 1999

Request Permission or Order Reprints Instantly!